Appl. Sci. Converg. Technol. 24(6): 257-261 (2015)
http://dx.doi.org/10.5757/ASCT.2015.24.6.257

Research Paper

Investigation of detection wavelength of Quantum Well Infrared-Photodetector

S. H. Hwang, J. G. Lim, J. D. Song, J. C. Shin, D. C. Heo, and W. J. Choi*

Center for Opto-Electronics Materials and Devices, Korea Institute of Science and Technology (KIST), Hwarangno 14-gil 5, Seongbuk-gu, Seoul 136-791, Korea

Received October 22, 2015; accepted November 9, 2015

Abstract We report on GaAs/AlGaAs quantum well infrared photodetectors (QWIPs) that can cover the spectral range of 3.6-25 μm. One advantage of the GaAs QWIPs is the wavelength tenability as a function of their structural parameters. We have performed a systematic calculation on the detection wavelength of a typical GaAs/$Al_xGa_{1-x}As$ multi-quantum-well photodetector, with the aluminum mole fraction (x) of $Al_xGa_{1-x}As$ barrier in the range of 0.15- 0.43 and the quantum-well width range from 30 to 60 Å. Design and fabrication of a QWIP based on GaAs/$Al_{0.23}Ga_{0.77}As$ structure with 37 Å-thick well width has been carried out. The calculated operation wavelength of the QWIP is in a good agreement with the experimental data taken by photo response and activation energy calculation from thermal quenching of integrated photoluminescence.

Keywords: Quantum well, Infrared, Photodetector, QWIP

I. Introduction

Mid to far infrared (IR) wavelength technology has found its use in a lot of applications. These include military, medical imaging, environmental monitoring, and astronomy observations, etc [1-3]. It should be noted that both tactical and strategic uses of IR imaging systems require the availability of high performance detector arrays operating at wavelengths within and beyond the 10-18 μm spectral band. In order to detect this type of radiation, various types of material have been studied and are practically used. In the past, the limited choice of semiconductors (e.g., Si, Ge, InSb) had restricted the operation wavelength range of the IR radiation. As the semiconductor technology matures, narrow gap materials such as HgCdTe have been used for the l-10 μm detector. However, they have disadvantages such as the difficulty in the control of uniformity, which is a drawback for the fabrication of detector array. Recently, several researchers have proposed a method of IR detection based upon the photo-excitation of carriers out of a quantum well (QW), either by an intersubband-like transition or through enhanced free-carrier absorption [4-5]. This quantum well infrared detector (QWIP) might be preferable to the narrow bandgap detector or Schottky barrier detector for the FIR wavelength range, since QWIPs have shown better characteristics in the fabrication, the detection threshold and the quantum efficiency. Large oscillator strengths in intersubband transitions have been evidenced for the first time by West and Eglash [6]. These intersubband transitions have been given birth to a wealth of new IR devices [7-8].

When QW has one electron state in conduction band, the confined electrons in a doped QW can be excited to continuum states by the absorption of IR photons. The photo-excited electrons then transport through vertically, therefore producing a photocurrent. One of materials for QWIP is GaAs/AlGaAs system. Comparing with HgCdTe detectors, GaAs/AlGaAs QWIP has a number of advantages, such as higher device uniformity due to mature material growing technologies, monolithic integration with high performance GaAs electronics, and easy control of the detection wavelength by controlling the QW parameters [7-14].

In this work, we present a theoretical consideration of the operation energy corresponding to the maximum absorption wavelength of the QWIPs with QW parameters. The QWIPs considered in this work are the single bounded-state detectors (bound-to-continuum transition) consisting of a number of QWs separated by thick barriers. The QWs are separated far apart so that the energy levels in each well are decoupled from the other wells and can be treated independently [15]. The theoretically calculated operation wavelength of QWIP is compared with those determined by the spectral response of fabricated QWIP and the activation energy obtained from integrated photoluminescence (PL) intensities.

---

*Corresponding author
E-mail: wjchoi@kist.re.kr

II. GaAs/AlGaAs QWIP Design

The design of QWIP is based on widely accepted models. The bound states in GaAs/AlGaAs QW have been calculated in order to determined the interband transition energy and the intersubband transition energy by using the envelope function approximation and the 8 band k・p model for describing the well and barrier layers [16]. The energy states of the conduction are calculated with the above model. We used the model suggested in Ref. 15 to calculate the continuum levels.

For the calculation, bound-to-continuum transition, which means that there is only one bound state in the QW conduction band, has been assumed. In this case, the operation wavelength of QWIP results from the transition between the ground state in the QW conduction band and the continuum state [17]. It has been also assumed that the maximum IR absorption is occurred at the same IR photon energy that gives the maximum electrical responsivity and conduction band offset between GaAs and AlGaAs is insensitive to temperature.

Fig. 1 shows the calculated bound-to-continuum transition energies as a function of the quantum well width for various Al mole fractions in the AlGaAs barrier regions. As mentioned earlier, the model suggested in Ref. 15 is used to calculate the continuum levels. The interband transition energy and the intersubband transition energy by using the envelope function approximation and the 8 band k²p model for describing the well and barrier layers are also used [16]. In this work, the Al mole fraction of the AlGaAs barrier was varied from 0.15 to 0.43 and the quantum well width was varied from 30 to 60 Å in order to cover the spectral range from 3.6 to 25 μm (50~340 meV). One can consider the calculated bound-to-continuum transition energy as the peak IR detection energy in QWIP. The transition energy increases with the wider GaAs well width and the larger Al mole fraction in AlGaAs barrier due to the enhanced quantum confinement effect. Therefore, one can design GaAs/AlGaAs QWIPs for specific IR wavelengths by choosing proper GaAs well widths and Al mole fraction in AlGaAs barrier.

As one can see in Fig. 1, for the $Al_{0.15}Ga_{0.85}As$ barrier, the GaAs well width should be smaller than 60 Å, so that GaAs well should have only one bound state in the conduction band. Since the barrier height is higher for larger Al mole fraction in AlGaAs barrier, the well width to permit single electron bound state is reduced. For example, the $Al_{0.43}Ga_{0.57}As$ barrier needs GaAs well width smaller than 30 Å for a single electron bound state. There is an increase in transition energy of ~50 meV for the increase of Al mole fraction from 0.15 to 0.19 (27% increase) with a GaAs well width of 30 Å. The same amount of transition energy shift can be obtained with the increase of GaAs well width for $Al_{0.15}Ga_{0.85}As$ barrier from 30 Å to 60 Å (100% increase). Therefore one can conclude that the detection wavelength of GaAs/AlGaAs QWIP is much sensitive to Al mole fraction of AlGaAs barrier layer than GaAs well width.

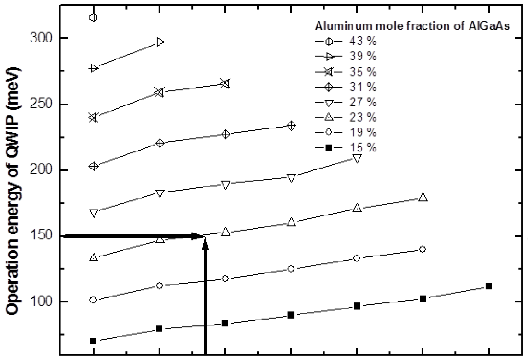

Figure 1. The operation energy of QWIP with various Al mole fractions and well width of GaAs.

III. Experiment and Measurement

The QWIP structure has been grown on a semi-insulating (100) GaAs substrate by metal organic chemical vapor deposition (MOCVD) method in order to verify the validity of the QWIP design. Fig. 2 shows GaAs/$Al_{0.23}Ga_{0.77}As$ QWIP structure used in this study. The QWIP structure has 25 periods of GaAs (3.7 nm)/$Al_{0.23}Ga_{0.77}As$ (50 nm) QWs which were designed to accommodate only one confined state in conduction band for a bound to continuum transition and to have 8.26 μm (150 meV) of operational wavelength as shown in Fig.1 marked with arrows. The GaAs QW region was doped with Si to $2{\times}10^{18}$ cm^{-3} in order to provide electrons in the QWs for absorption. The thickness of $Al_{0.23}Ga_{0.77}As$ barrier was set to 50 nm to prevent carrier leakage and state coupling between adjacent QWs.

The QWIP substrate was processed using standard photolithography, wet etching and metal evaporation. A H_3PO_4:H_2O_2:H_2O solution was used for a mesa etching and E-beam evaporated Ti/Au was used for contact metals. The pixel size of the QWIP was 200×200 μm². One side of the sample edge was polished at an angle of 45° in order to

Layer	Materiel System	Thickness	
Contact	GaAs Nd=2 x 10 cm^{-3}	0.5 μm	
Barrier	$Al_{0.23}Ga_{0.77}As$	50 nm	X 25 periods
Well	GaAs Nd=2 x 10 cm^{-3}	3.7 nm	
Barrier	$Al_{0.23}Ga_{0.77}As$	50 nm	
Contact	GaAs Nd=2 x 10 cm^{-3}	1 μm	
Substrate	S.I-GaAs		

Figure 2. Schematic diagram of quantum well infrared photodetector structure.

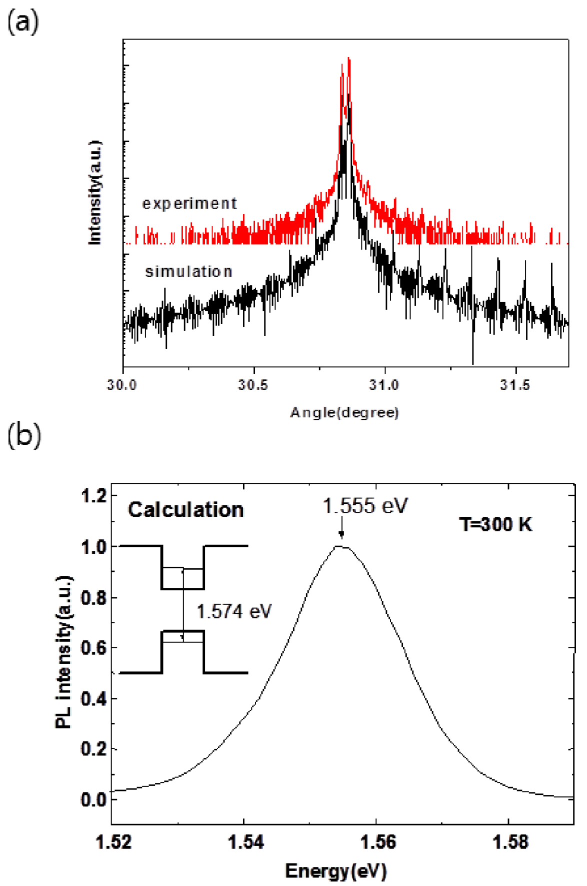

Figure 3. (a) X-ray data simulation and experiment data (b) 300 K-PL spectrum.

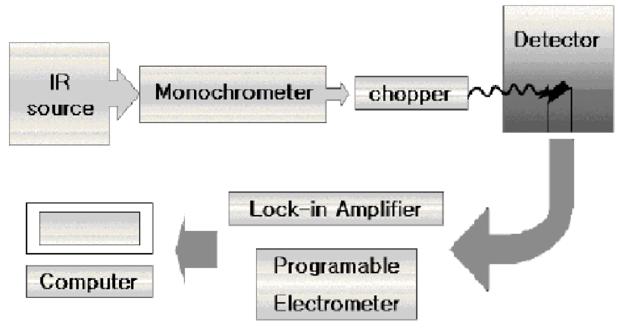

Figure 4. The measurement system of QWIP.

satisfy the selection rule of the inter-subband transition in the QW. The spectral response of the fabricated QWIP was measured at 10 K using the measurement setup described in Fig. 4.

High resolution double crystal X-ray diffraction measurement and 300 K-PL measurement have been adopted as a nondestructive method to precisely determine the structure parameters, such as the Al mole fraction in AlGaAs barrier layer and the GaAs well width. Integration of PL spectra as a function of measurement temperature and 300 K-PL spectrum were taken by 1 m-long monochromater, 514.5 nm Ar ion lasers and liquid N_2 cooled InGaAs detectors in close-cycled He cooled cryostat.

IV. Results and Discussion

One can find structure parameters of GaAs/$Al_xGa_{1-x}As$ MQW from X-ray diffraction data. The highest peak position and the interval angle of other satellite peak position from X-ray experiment data can give the well width and barrier width as well as the Al mole fraction (x) of GaAs/$Al_xGa_{1-x}As$ MQW. The calculation of X-ray diffracted rocking curves for the mutli-QW structure has been carried out for the structure illustrated in Fig. 2 by solving Takaki-Taupin differential equation based on the dynamical theory [18]. Figure 3(a) shows the experimental and calculated rocking curves for the X-ray diffraction of the QWIP structure. The excellent agreement between the experimental data and calculation data confirms the precise control in the growth of multi-QW structure used in the work.

Fig. 3(b) shows the PL spectrum of the sample measured at room temperature. The peak position of PL spectrum corresponds to carrier transition energy from the fundamental state of the conduction band to that of the valence band. The calculation of inter-band transition was carried out by using the method described in section II. The transition energy determined by PL spectrum was 1.555 eV, which is agreed well with the calculation value of 1.574 eV. This result also confirms the precise control in the growth of mulit-QW structure.

Figure 5 shows that the photo response spectra for the sample were measured at 10 K under the positive bias voltage of 1 V with a measurement setup described in Fig. 4. The peak wavelength in spectral response of QWIP was 151.2 meV (=8.2 μm), which is also excellent agreement with the calculation value, 150.0 meV (=8.26 μm).

It is well known that integrations of PL of QWs and quantum dots are thermally quenched and the activation energies abstracted from it is related to the confined states of the QWs or the quantum dots [19-21]. Considering each level of the QWs as an independent trap of electrons in the conduction band of the QW, a detraping rate can be described

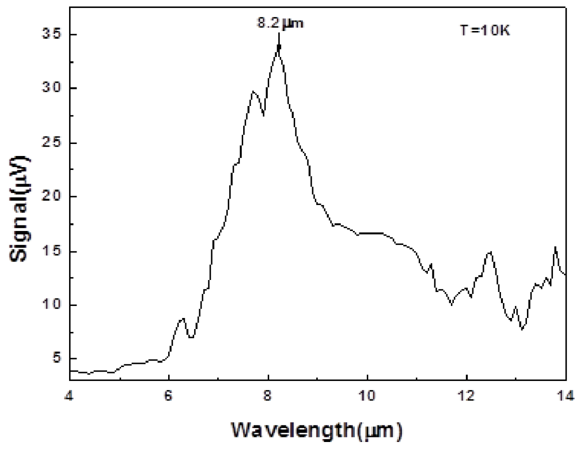

Figure 5. Spectral response of QWIP at T=10 K.

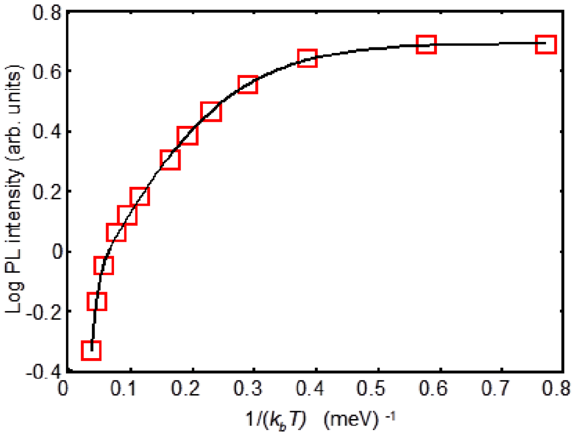

Figure 6. Integrated PL as a function of measurement temperature (open box) and fitting curve for the activation energy (solid line).

as exp$(-\Delta DE/k_BT)$ (activation energy $\Delta DE = E_{barrier}\text{-}E_{trap}$, Boltzmann's constant k_B, measured temperature T) [20]. Therefore, thermionic processes with two activation energy levels in the conduction band are modeled by the following equations [21].

$$I_{PL}=I_0/[1+n_1 exp(-E_d/k_BT)+n_2 exp(-E_d/k_BT)] \qquad (1)$$

where, I_{PL}, E_a, E_b, k_B and T stand for integration of measured PL, activation energies between each bounded level (meV) and the AlGaAs barrier, Boltzmann's constant (8.62×10^{-2} meV/K), and measured temperature (K), respectively. I_0, n_1 and n_2 represent excitation rate in the barrier and the fitting constants. Integrated PL intensity as a function of measurement temperature is illustrated in Fig. 6 (open box). The fitted activation energies with equation (1) and experimental data are E_a=144.201±37.72 meV and E_b=10.3956±0.2176 meV and we can find that the fitted solid line in Fig. 6 agree well with measured data. It is notable that the activation energy of E_a is close to calculated data (150 meV) and peak energy of photo response (151.2 meV). The origin of E_b is not clear at this moment. However, we can consider a defect level in AlGaAs barriers or interfaces between GaAs and AlGaAs.

In this study, the operation energy was calculated to be 150 meV (=8.26 μm). This energy is corresponding to the maximum absorption coefficient. The photo response and the integrated PL have been carried out to know the operation energy experimentally and they were compared with the value from the calculation. The experimental peak absorption energy from the photo response was 151.2 meV (=8.2 μm). The measurement of the photo response was carried out by 1 bias voltage and this bias could affect the potential barrier height [24]. This bias voltage made the potential barrier height lower. On the contrary, the bound energy state could be lower a little due to relatively low field (=7.18 kV/cm) corresponding to 1 bias voltage with a simple second-order perturbation theory [25]. Therefore, the operation absorption energy from difference between the bound state and the continuum state is expected to be decreased.

Integration PL has as a function of measurement temperature been measured and the activation energy was fitted to be 144±37.72 meV. This fitting value was the activation energy, which was corresponding to the operation energy of QWIPs due to the structure where there is only one bound state in the conduction band. This operation energy from calculation was within error range of the fitting value considering the bound-exciton complex [22,23].

V. Conclusions

Designs, Fabrication and Measurement of QWIPs based on GaAs/AlGaAs materials have been carried out. The design of QWIP has been based on "bound to continuum transition" so that QWIP structure has been designed to have only one bound state in the conduction band. The absorption coefficients from the bound state to the continuum state have been calculated and the maximum value has been considered to be the operation energy of QWIPs. Photo response and integrated PL have been investigated to compare the experimental values with the calculated one and have a good agreement among the values.

Acknowledgments

This work was supported by the Technology Innovation Program (10053010, Development of mid-IR quantum cascade lasers for portable high sensitivity(ppb) gas sensors) funded By the Ministry of Trade, industry & Energy (Korea) and partially by KIST institutional program. The authors thank S. W. Lee for fruitful discussions.

References

[1] R. L. Whitney, F. W. Adams, and K. F. Cuff, *Intersubband Transitions in Quantum Wells* (Plenum, New York, 1992) NATO ASI Series, B, p. 288.
[2] M. O. Manasreh, *Semiconductor Quantum Wells and Superlattices for Long Wave-length Infrared Detectors* (Artech House, Boston, 1993).
[3] E. H. Li, *Jpn. J. Appl. Phys*. 36, 3418 (1997).
[4] S. A. Lyon, *Preliminary Reports, Memoranda and Technical Notes* (Mater. Res. Council Summer Conf, La Jolla, July, 1982) p. 51.
[5] L. C. Chiu, J. S. Smith, S. Margalit, and A. Yariv, *Appl. Phys. Lett*. 43, 331 (1983).
[6] L. C. Wesh and S. J. Eglash, *Appl. Phys. Lett*. 46, 1156 (1985).
[7] J. S. Smith, L. C. Chiu, S. Margalit, A. Yariv, and A. Y. Cho, *J. Vac. Sci. Technol*. B 1, 376 (1983).
[8] B. F. Levine, K. K. Choi, C. G. Bethea, J. Walker, and R. J. Malik, *Appl. Phys. Lett*. 50, 1092 (1987).
[9] B. F. Levine, C. G. Bethea, K. K. Choi, J. Walker, and R. J. Malik, *J. Appl. Phys*. 64, 1591 (1988).
[10] B. F. Levine, C. G. Bethea, G. Hansnain, J. Walker, and R. J. Malik, *Appl. Phys. Lett*. 53, 296 (1988).

[11] G. Hansnain, B. F. Levine, C. G. Bethea, R. F. Logan, J. Walker, and R. J. Malik, *Appl. Phys. Lett*. 54, 2515 (1989).

[12] C. G. Bethea, B. F. Levine, G. Hansnain, J. Walker, and R. J. Malik, *J. Appl. Phys*. 66 July 15 (1989).

[13] D. D. Coon and R. P. G. karunasiri, *Appl. Phys. Lett*. 45, 649 (1984)

[14] D. D. Coon, R. P. G. karunasiri, and H. C. Liu, *J. Appl. Phys*. 60, 2636 (1986).

[15] K. K. Choi, *J. Appl. Phys*. 73, 5230 (1993).

[16] G. Bastard, *Wave Mechanics Applied to Semiconductor Heterostructures* (Les Editions de Physique, Les Ulis, France, 1998).

[17] Y. Gusakov, E. Finkman, G. Bahir, and D. Ritter, *Appl. Phys. Lett*. 79, 2508 (2001).

[18] W. J. Bartels, J. Hornstra, and D. J. W. Lobeek, *Acta Crystalloge*, A 42, 539 (1986).

[19] J. D. Lambkin, D. J. Dunstan, K. P. Homewood, L. K. Howard, and M. T. Emery, *Appl. Phys. Lett.* 57, 1986 (1990).

[20] M. Vening, D. J. Dunstan, and K. P. Homewood, *Phys. Rev. B* 48 (1993) 2412.

[21] S. –K. Park, Y. J. Park, E. K. Kim, C. J. Park, H. Y. Cho, Y. S. Lim, J. Y. Lee, and C. Lee, *Jpn. J. Appl. Phys.* 41 (2002) 4378.

[22] F. E. Wiliams and H. J. Erying, *J. Chem. Phys*. 15, 289 (1947).

[23] D. Bimberg and M. Sondergeld, *Phyica. Rev. B* 4, 3451 (1971).

[24] E. Pelve, F. Beltram, C. G. Bethea, B. F. Levine, V. O. Shen, S. J. Hsieh, and R. R. Abbott, *J. Appl. Phys*. 86, 5656 (1989).

[25] M. Matsuura and T. Kamizato, *Phys. Rev*. B 33, 8385-8389 (1986).